

Excited states of the free excitons in CuInSe₂ single crystals

M. V. Yakushev,^{1,a)} F. Luckert,¹ C. Faugeras,² A. V. Karotki,³ A. V. Mudryi,³ and R. W. Martin¹

¹Department of Physics, SUPA, Strathclyde University, G4 0NG Glasgow, United Kingdom

²LNCMI, CNRS, UJF, UPS, INSA, BP 166, 38042 Grenoble Cedex 9, France

³Scientific-Practical Material Research Centre of the Belarus National Academy of Science, P.Brovki 19, 220072 Minsk, Belarus

(Received 27 August 2010; accepted 25 September 2010; published online 14 October 2010)

High-quality CuInSe₂ single crystals were studied using polarization resolved photoluminescence (PL) and magnetophotoluminescence (MPL). The emission lines related to the first ($n=2$) excited states for the A and B free excitons were observed in the PL and MPL spectra at 1.0481 meV and 1.0516 meV, respectively. The spectral positions of these lines were used to estimate accurate values for the A and B exciton binding energies (8.5 meV and 8.4 meV, respectively), Bohr radii (7.5 nm), band gaps ($E_g^A=1.050$ eV and $E_g^B=1.054$ eV), and the static dielectric constant (11.3) assuming the hydrogenic model. © 2010 American Institute of Physics. [doi:10.1063/1.3502603]

Solar cells with CuInSe₂-based absorber layers are the leading thin-film technology in terms of conversion efficiencies, reaching 20%,¹ and stability. CuInSe₂ has a direct band gap near 1.05 eV and an absorption coefficient exceeding 10^5 cm⁻¹, one of the highest among known semiconductors. Despite a considerable amount of research the evolution of the conversion efficiency is showing a tendency to saturate well below the theoretical limit of about 30% for a one-junction solar cell² suggesting a lack of fundamental understanding of these materials.

A key milestone in the understanding and application of every semiconductor material is the unambiguous observation of free excitons and their excited states. Resolving both the ground and excited states of the free excitonic transitions is a reliable way to accurately determine such parameters as the band-gap (E_g).³ Despite many studies of the optical properties of CuInSe₂ dating back nearly 40 years⁴ only very few reports suggest resolution of the A and B free excitonic states.^{5–8} No reliable information on their excited states has yet been reported and therefore the band-gap cannot be considered to be accurately known.

Previous experimental attempts to determine the free exciton binding energies E_b in CuInSe₂ have been carried out by analyzing either the temperature quenching of the excitonic photoluminescence (PL) emission intensity^{7,9} or diamagnetic shifts under the influence of magnetic fields.¹⁰ The quenching characteristics of the A and B excitons are rather complex due to the small energy splitting and proximity of shallow bound excitons and thus values of E_b determined by this method cannot be considered as reliable. The technique based on the analysis of the exciton line diamagnetic shift is valid within the weak field approximation, which limits the accuracy of E_b .^{10,11} These issues are reflected in the considerable scatter of the E_b^A values in the literature, ranging from 4.3 to 39.1 meV (Refs. 6, 7, 9, 10, and 12–14) resulting in scattered values of the band gap. It is advantageous to determine E_b from the spectral positions of the PL lines of the free exciton ground and excited states as this does not involve

any other material parameters. This gives one an opportunity to clarify the static dielectric constant ϵ , which also reveals a considerable scatter in the literature [from 16 (Ref. 15) to 9.3 (Ref. 16)], assuming published values of the effective masses are correct and the validity of the hydrogenic model.

In this letter, PL and reflectance (RF) data on CuInSe₂ bulk crystals, grown from the melt, are used to resolve a wide range of excitonic transitions, including the A and B free excitonic excited states. The quality of the crystal is demonstrated by the improved resolution and intensity of the free excitonic transitions. Polarization and magnetic field dependent spectra are used to probe the symmetry and clarify the assignments. The spectral positions of PL lines related to excited states were used to calculate accurate values of the band gap and dielectric constant, as well as the binding energies, and Bohr radii (a_B) of the A and B free excitons in CuInSe₂.

Bulk single crystals of CuInSe₂ were cleaved from the middle part of an ingot grown by the vertical Bridgman technique using a near stoichiometric mix of the high purity elements Cu, In, and Se.¹⁷ The elemental composition of the crystals, measured by energy dispersive X-ray analysis (EDX) was close to ideal stoichiometry (Cu: 24.9, In: 24.9, and Se: 50.2 at. %). The orientation of the three major cubic structure crystallographic axes $\langle 001 \rangle$, $\langle 010 \rangle$, and $\langle 100 \rangle$ of the samples was established by analysis of x-ray Laue patterns. Cleaved surfaces of the crystals were examined using PL and RF at 6 K at Strathclyde and magneto-PL (MPL) at 4.2 K at the Grenoble High Magnetic Field Laboratory (GHMFL). Magnetic fields up to 20 T were directed perpendicular to c ($B \perp c$), which is the tetragonal distortion direction in the crystalline lattice. Both the PL and the MPL measurements employed the unpolarized 514 nm line of an Ar⁺ laser as an excitation source while the RF measurements used a 100 W tungsten halogen lamp. The spectral resolution was determined as 0.07 meV for the RF, 0.8 meV for the polarization resolved PL at 6.5 K, and 0.14 meV for the PL and MPL at 4.2 K. The spectral position of the lines was determined with an accuracy of 0.2 meV. More details on the experimental set ups can be found elsewhere.^{9,10,12}

The near band gap region of the PL and RF spectra taken in CuInSe₂ at 4.2K and 6K, respectively, using nonpolarized

^{a)}Author to whom correspondence should be addressed. Electronic mail: michael.yakushev@strath.ac.uk.

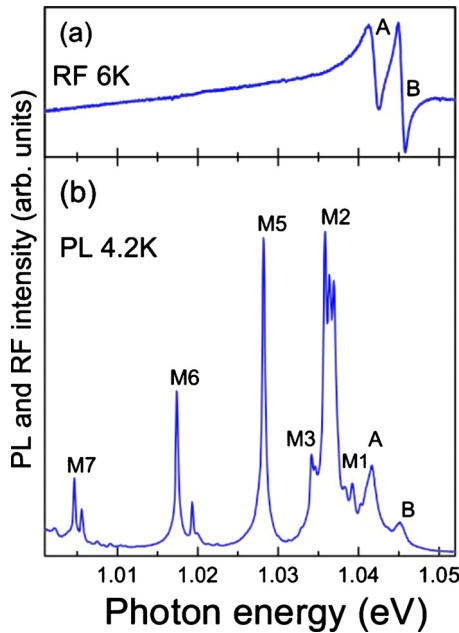


FIG. 1. (Color online) Near band-gap regions in (a) RF and (b) PL spectra for CuInSe₂ single crystals taken at 6 K and 4.2 K, respectively, showing lines of free and bound excitons.

light, are shown in Figs. 1(a) and 1(b), respectively. The RF spectrum reveals two prominent resonances, associated with the A and B free excitons, confirming that the lines at 1.0417 eV and 1.0453 eV in the PL spectra are related to the A and B free excitons, respectively.^{7,8} The A exciton energy, determined in this paper (1.0417 eV), is very close to that reported by Chatrohorn *et al.*⁷ for single crystals (1.0418 eV) but higher than the values measured by Schön *et al.*⁶ for single crystals (1.0406 eV) and Niki *et al.*⁵ for epitaxial layers (1.0386 eV). The difference can be explained by the influence of intrinsic defects due to deviations from the ideal stoichiometry¹⁹ and strain in the epitaxial layer due to a mismatch in the CuInSe₂ and GaAs lattice parameters.⁸ In addition to the free exciton lines the spectrum shows several well resolved lines M1–M7 which have been previously attributed to bound excitons and their excited states.^{7–9}

The chalcopyrite structure of CuInSe₂ can be derived from the sphalerite zinc blende structure of ZnSe by the ordered replacement of Zn either with Cu or In. These two nonequivalent replacements result in two different lengths for the chemical bonds Cu–Se and In–Se creating a tetragonal distortion¹⁸ splitting the triply degenerated valence band at the Γ point of the Brillouin zone in ZnSe into the three sub-bands A, B, and C. In terms of the quasicubic model²⁰ this splitting can be described as the simultaneous influence of the noncubic crystal-field and spin-orbit interactions, which in CuInSe₂ determine the spectral splitting of the A-B and B-C bands, respectively. The tetragonal distortion τ , given by $1 - c/2a$, where c and a are the lattice constants, has a small negative value (-0.52%) in the samples studied here. This results in a small and positive value of the crystal field splitting (Δ_{cf}), which inverts the valence sub-band sequence in CuInSe₂ and gives the uppermost A sub-band the Γ_{6v} symmetry.

The region of the free excitonic transitions is examined more closely using PL spectra measured with a linear polarizer oriented either along ($E\parallel c$) or perpendicular ($E\perp c$) to

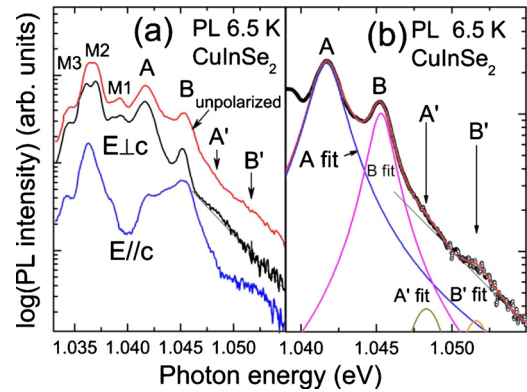


FIG. 2. (Color online) (a) Near band-gap regions in PL spectra for CuInSe₂ single crystals taken at unpolarized, polarized $E\perp c$ and $E\parallel c$ conditions at 6 K (offset for clarity); (b) the A and B free exciton region of the unpolarized PL spectra in CuInSe₂ single crystals fitted with A, B, A', and B' Lorentz shape curves.

the c —axis of the crystalline lattice as shown in Fig. 2(a). The A and B free exciton transitions are resolved at 1.0417 and 1.0453 eV in the unpolarized spectrum.^{7,8}

It is clear that the A free exciton emission is predominantly polarized $E\perp c$, reaching a maximum intensity I_{\perp}^A at this polarization as reported for electro-reflectance²¹ and PL (Ref. 22) spectra. This is consistent with the selection rules for an A excitonic transition involving the Γ_{6v} symmetry of the top valence sub-band and the Γ_{6c} symmetry of the conduction band. According to the quasi-cubic model,²⁰ the theoretical ratio of $I_{\perp}^A/I_{\parallel}^A$ intensities should reach 9.²¹ In our PL experiment the value of $I_{\perp}^A/I_{\parallel}^A$ is 7.1, approaching the theoretical value more closely than the earlier reported value of 5 for electroreflectance.²¹ The B exciton line does not change as dramatically with polarization as the A exciton line. Its intensity is almost unchanged, which is consistent with the selection rules for a transition between the Γ_{7v} symmetry B valence sub-band and the Γ_{6c} symmetry conduction band for both the $E\perp c$ and $E\parallel c$ polarizations.²¹ However, it is noted that its width is reduced from about 2.2 meV in the nonpolarized spectrum down to 1.1 meV for the $E\perp c$ polarization.

The lines related to the excited states (A' and B') of the free excitons become visible to higher energy in Fig. 2. Their intensities are weak but the polarized spectra aid their identification. For the $E\parallel c$ polarization the reduced strength of the A exciton ground and excited transitions improves the visibility of the excited state line of the B exciton and also clarifies the A' ($n=2$) contribution to the high-energy tail of the B exciton line. Conversely, for the $E\perp c$ polarization, the narrowing of the B exciton line allows the line related to the A' excited state, to be more clearly resolved as shown in Fig. 2(a). The straight line emphasizes its presence.

The excited state lines can also be seen in the unpolarized PL spectra taken at higher excitation density as shown in Fig. 2(b). In particular the separation of B' from the other lines allows it to be resolved more clearly, whereas A' is not so well resolved due to the proximity of the B line. In order to determine their spectral positions this unpolarized PL spectrum has been fitted with Lorentz shape curves of A, B, A', and B'. The spectral positions of the excitonic lines fitted with Lorentzians are shown in Table I. Further evidence for the excited state nature of the weaker features A' and B' in the PL spectra is provided by the MPL spectra in Fig. 3(a). The spectra show the B exciton lines shifting toward higher

TABLE I. The spectral positions of the excitonic lines fitted with Lorentzians.

Excitons	A	B	A'	B'
$h\nu$ (eV)	1.0417	1.0453	1.0481	1.0516

energies and splitting into two components. At higher energies the spectra also reveal components of the A' and B' ($n=2$) excited states. These features are more easily seen at magnetic fields above 2 T, for which the effective exciton size and the Bohr radius are reduced. In addition the field causes an increase in binding energy, rendering the excitons more stable. The dependence of the spectral positions of the B ($n=1$), A', and B' ($n=2$) lines on the magnetic field at $B \perp c$ are shown in Fig. 3(b). The A' line is seen to split noticeably into two components, which converge to 1.0481 eV as the field reduces to zero. At 2 T the B' line, related to the excited state, can also be seen in Fig. 3(a). According to the hydrogenic model for simple parabolic bands in a direct band gap material the spectral position $E(n)$ of a free exciton line in the n^{th} excited state is, as follows:¹¹

$$E(n) = E_g - E_b = E_g - 13.6 \frac{\mu}{m_0 \varepsilon^2 n^2}, \quad (1)$$

where $\mu = m_e m_h / m_e + m_h$ is the reduced mass of exciton, m_0 is the free electron mass, m_e is an effective electron, and m_h an effective hole masses, and ε is the static dielectric constant of the material. From the spectral separation of the ground ($n=1$) and excited ($n=2$) states, shown in Table I, the binding energies of the A and B excitons have been calculated using the formula

$$E_b = \frac{4}{3} [E_{\text{FE}}(n=2) - E_{\text{FE}}(n=1)], \quad (2)$$

and are shown in Table II. Accurate values of the A and B band gaps are also calculated using $E_g = E(n=1) + E_b$ and shown in Table II. Assuming literature values of the effective masses for the electron and hole in CuInSe₂ ($m_e = 0.09m_0$ and $m_h = 0.71m_0$, respectively²³), the static dielectric constant in CuInSe₂ was calculated to be $\varepsilon = 11.3$ using Eq. (1). The Bohr radii for the A and B free excitons have also been calculated as: $a_B = a_B^H m_0 \varepsilon / \mu$, where a_B^H is the Bohr radius for

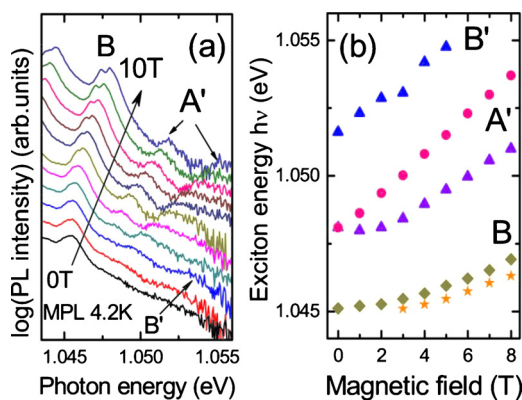


FIG. 3. (Color online) (a) The evolution of the B ground ($n=1$) state exciton and the A' and B' excited ($n=2$) states under the influence of magnetic fields at $B \perp c$, (b) dependence of the spectral positions of the lines related to the ground B and A' and B' excited states of free excitons on the magnetic field strength.

TABLE II. The band gaps, binding energies E_b , and Bohr radii a_B of the A and B excitons.

Excitons	E_b (meV)	a_B (nm)	E_g (eV)
A	8.5	7.5	1.0502
B	8.4	7.5	1.0537

hydrogen. The calculated values of a_B are shown in Table II.

In conclusion, high quality CuInSe₂ single crystals were studied by PL spectroscopy, employing polarization and magnetic field dependence to clarify the properties of the free exciton transitions. The lines related to the first ($n=2$) excited states for the A and B free excitons at $E_A(n=2) = 1.0481$ eV and $E_B(n=2) = 1.0516$ eV, respectively, have been observed in the PL and MPL spectra. Accurate values of the A and B exciton binding energies $E_b^A = 8.5$ and $E_b^B = 8.4$ meV have been established. These are then used to estimate Bohr radii a_B of 7.5 nm for both excitons, a 6 K band gap of 1.050 eV for the A exciton and of 1.054 eV for the B exciton as well as the value of 11.3 for the static dielectric constant. A standard hydrogenic model is assumed.

This work was supported by the EPSRC (Grant No. EP/E026451/1), the Royal Society (Grant No. IJP 2008/R1), BCFR (Grant No. F09MC-003), "Nanomaterials and nanotechnology" (6.17), and EC-EuroMagNetII-228043.

¹I. Repins, M. A. Contreras, B. Egaas, C. DeHart, J. Scharf, C. L. Perkins, B. To, and R. Noufi, *Prog. Photovolt. Res. Appl.* **16**, 235 (2008).

²W. Shockley and H. J. Queisser, *J. Appl. Phys.* **32**, 510 (1961).

³M. Smith, G. D. Chen, J. Y. Lin, H. X. Jiang, M. A. Khan, C. J. Sun, Q. Chen, and J. W. Yang, *J. Appl. Phys.* **79**, 7001 (1996).

⁴J. L. Shay and J. H. Wernick, *Ternary Chalcopyrite Semiconductors-Growth, Electronic Properties, and Applications* (Pergamon, New York, 1975).

⁵S. Niki, H. Shibata, P. J. Fons, A. Yamada, A. Obara, Y. Makita, T. Kurafuji, S. Chichibu, and H. Nakanishi, *Appl. Phys. Lett.* **67**, 1289 (1995).

⁶J. H. Schön and E. Bucher, *Appl. Phys. Lett.* **73**, 211 (1998).

⁷S. Chatrathorn, K. Yoodee, P. Songpongs, C. Chityuttakan, K. Sayavong, S. Wongmanerod, and P. O. Holtz, *Jpn. J. Appl. Phys., Part 2* **37**, L269 (1998).

⁸A. V. Mudryi, I. V. Bodnar, I. A. Viktorov, V. F. Gremenok, M. V. Yakushev, R. D. Tomlinson, A. E. Hill, and R. D. Pilkington, *Appl. Phys. Lett.* **77**, 2542 (2000).

⁹M. V. Yakushev, R. W. Martin, and A. V. Mudryi, *Phys. Status Solidi C* **6**, 1082 (2009).

¹⁰M. V. Yakushev, R. W. Martin, A. Babinski, and A. V. Mudryi, *Phys. Status Solidi C* **6**, 1086 (2009).

¹¹C. F. Klingshirn, *Semiconductor Optics* (Springer, New York, 1997).

¹²M. V. Yakushev, Y. Feofanov, R. W. Martin, R. D. Tomlinson, and A. V. Mudryi, *J. Phys. Chem. Solids* **64**, 2011 (2003).

¹³M. A. Abdulaev, *Sov. Phys. Semicond.* **26**, 1196 (1992).

¹⁴L. Nemerenco, *Moldavian J. Phys. Sci.* **4**, 438 (2005).

¹⁵G. Riede, H. Subotta, H. Neumann, and X. N. Hoang, *Solid State Commun.* **28**, 449 (1978).

¹⁶P. W. Yu, *J. Appl. Phys.* **47**, 677 (1976).

¹⁷R. D. Tomlinson, *Sol. Cells* **16**, 17 (1986).

¹⁸J. E. Jaffe and A. Zunger, *Phys. Rev. B* **29**, 1882 (1984).

¹⁹M. V. Yakushev, A. V. Mudryi, and R. D. Tomlinson, *Appl. Phys. Lett.* **82**, 3233 (2003).

²⁰J. E. Rowe and J. L. Shay, *Phys. Rev. B* **3**, 451 (1971).

²¹J. L. Shay, H. M. Tell, H. M. Kasper, and L. M. Schiavone, *Phys. Rev. B* **7**, 4485 (1973).

²²K. Hönes, M. Eickenberg, S. Siebentritt, and C. Persson, *Appl. Phys. Lett.* **93**, 092102 (2008).

²³H. Neumann, *Sol. Cells* **16**, 317 (1986).